Available online at www.sciencedirect.com
ScienceDirect
Journal of Power Sources 172 (2007) 468–475
JOURNAL OF POWER SOURCES
www.elsevier.com/locate/jpowsour

# Ageing behaviour of electrochemical double layer capacitors Part I. Experimental study and ageing model

Oliver Bohlen *, Julia Kowal, Dirk Uwe Sauer

*Institute for Power Electronics and Electrical Drives ISEA, RWTH Aachen University, Aachen, Germany*

Received 14 May 2007; received in revised form 18 June 2007; accepted 2 July 2007
Available online 17 July 2007

**Abstract**

Different types of commercially available electrochemical double layer capacitors (EDLCs) were analysed in accelerated ageing tests by impedance spectroscopy. From these measurements the parameters of an impedance model were determined. The characteristic change of the impedance parameters is discussed and an ageing model for EDLCs is developed.


*Keywords:* Electrochemical double layer capacitor (EDLC); Supercapacitor; Ageing; Electrochemical impedance spectroscopy (EIS); State of health (SOH)

## 1. Introduction

Electrochemical double layer capacitors (EDLC), often called supercapacitors or ultracapacitors, are currently discussed as a high power storage device, especially for automotive applications [1]. Though having poor volumetric and gravimetric energy density compared with batteries, they are an interesting option for applications where charging or discharging with high current rates is needed for only a few seconds. Moreover, EDLCs outperform nearly any battery technology in terms of cycle life and could potentially live as long as the applications they are used in [2,3].

However, it is a mistake to believe that ageing of supercapacitors is not an issue. Even though energy storage in EDLCs is purely electrostatic, parasitic electrochemical reactions, such as the decomposition of the electrolyte, occur and can under certain circumstances drastically reduce the life expectancy of these devices. The two predominant factors that influence ageing are temperature and voltage. Both increased voltage and temperature exponentially accelerate electrochemical reactions [4–6]. Thus, understanding the impact of temperature and voltage on the ageing of EDLCs and being able to predict their effect on performance and lifetime quantitatively is essential for good system design.

## 2. Impedance model of an EDLC

The electrical behaviour of EDLCs can be described well by impedance-based models. Very basic capacitor models comprising an ideal capacitor in series with an internal resistance yield reasonable results for many applications [7], but fail to describe the dynamic behaviour precisely. These models can be extended by a series inductance to represent the stray inductance of the electrodes and connectors and a resistance in parallel to the capacitance as a first-order approximation for the leakage current [8].

### 2.1. Standard pore impedance

The most important improvement to this simple, linear model is the introduction of a pore impedance [9]. Porous electrodes show a behaviour that deviates noticeably from that of flat electrodes. The ion-conducting path from the bulk electrolyte towards a section of the double layer deep inside the pores of the electrode is longer than the path towards a section near the pore mouth. Thus, the series resistance varies depending on where the corresponding part of the double layer is inside the pore. The macroscopic effect of this spatially distributed impedance was described by de Levie [10].

* Corresponding author.
*E-mail addresses:* batteries@isea.rwth-aachen.de (O. Bohlen), batteries@isea.rwth-aachen.de (J. Kowal), batteries@isea.rwth-aachen.de (D.U. Sauer).
*URLs:* http://www.isea.rwth-aachen.de (O. Bohlen), http://www.isea.rwth-aachen.de (J. Kowal), http://www.isea.rwth-aachen.de (D.U. Sauer).

0378-7753/$ – see front matter © 2007 Elsevier B.V. All rights reserved.
doi:10.1016/j.jpowsour.2007.07.021

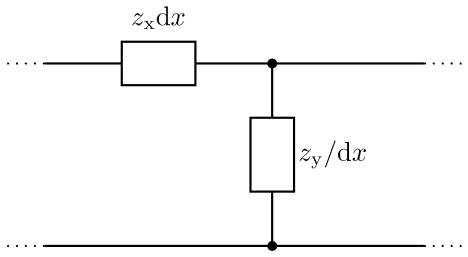


Fig. 1. Equivalent circuit of an infinitesimal pore section.

Fig. 1 shows an equivalent circuit of an infinitesimal fraction of the pore length. $z_x$ and $z_y$ are the impedance values per unit length of the pore along the pore axis ($x$) (assumed as perpendicular to the current collector) and perpendicular to the pore axis ($y$), respectively. As a first approach, the impedance along the pore axis is exclusively determined by the electrolyte conductivity $z_x\,\mathrm{d}x = \mathrm{d}R_{\mathrm{el}}$, while the impedance perpendicular to the pore axis and the pore walls is solely caused by the double layer capacitance $z_y^{-1}\,\mathrm{d}x = \mathrm{j}\omega\,\mathrm{d}C_{\mathrm{dl}}$. Integration along the pore axis yields an analytic expression for the pore impedance [11]:

$$Z_{\mathrm{p}} = \sqrt{\frac{R_{\mathrm{el}}}{\mathrm{j}\omega C_{\mathrm{dl}}}}\,\coth\sqrt{\mathrm{j}\omega R_{\mathrm{el}} C_{\mathrm{dl}}}. \tag{1}$$

For a uniform, long cylindrical cell, the values of $R_{\mathrm{el}}$ and $C_{\mathrm{dl}}$ can be calculated analytically from the geometry of the pore, the electrolyte conductivity and the properties of the double layer [10,11]. Eq. (1) can be approximated for high and low frequencies by

$$Z_{\mathrm{p}}(\omega \to \infty) \approx \sqrt{\frac{R_{\mathrm{el}}}{\mathrm{j}\omega C_{\mathrm{dl}}}} \tag{2}$$

and

$$Z_{\mathrm{p}}(\omega \to 0) \approx \frac{R_{\mathrm{el}}}{3} + \frac{1}{\mathrm{j}\omega C_{\mathrm{dl}}}, \tag{3}$$

respectively. Eq. (2) describes the typical branch with a constant phase angle of $\pi/4$ that can be seen in Fig. 2, left graph. The impedance for low frequencies equals that of an ideal capacitor with a series resistance, which reflects the fact that after a potential was applied to the pore impedance for a sufficiently long time, the current distributes equally on all capacitors $\mathrm{d}C_{\mathrm{dl}}$ and the corresponding resistors $\mathrm{d}R_{\mathrm{el}}$. One practical benefit of this pore model is that it can be approximated by finite ladder networks which can easily be implemented as a simulation model [9,12–15]. A good approximation can be already achieved with less than 10 RC-elements if the resistance values are determined by a least squares fit procedure from appropriate measurements [16]. Another simplification can be achieved by replacing the ladder network by a series connection of parallel RC-circuits [12,17].

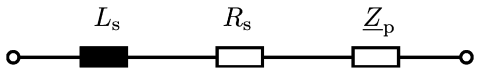


Fig. 3. Equivalent circuit of an EDLC.

An impedance model that accurately describes the behaviour of an EDLC over a wide frequency range can be achieved by extending this pore impedance with a series resistor $R_{\mathrm{s}}$ that models the ohmic resistance of conductors and the bulk electrolyte and an inductor representing the stray inductance of the device, as shown in Fig. 3[12,16,18]. The impedance of this standard model of an EDLC can be expressed as

$$Z_{\mathrm{EDLC,std}} = R_{\mathrm{s}} + \mathrm{j}\omega L_{\mathrm{s}} + \sqrt{\frac{R_{\mathrm{el}}}{\mathrm{j}\omega C_{\mathrm{dl}}}}\,\coth\sqrt{\mathrm{j}\omega R_{\mathrm{el}} C_{\mathrm{dl}}}. \tag{4}$$

Fig. 2 shows the impedance spectrum of this standard model that was fitted to the measured impedance spectrum of a commercial EDLC (EPCOS 600 F, 25 °C, 2.7 $V_{\mathrm{dc}}$). The left figure shows a Nyquist plot of the high- and medium-frequency range. The standard model describes very well the real behaviour in the frequency range above approximately 1 Hz. The main contribution to the impedance branch that describes a 45° angle to the real axis originates from the pore impedance $Z_{\mathrm{p}}$. The inductive behaviour dominates at frequencies above approx. 100 Hz. The real part of the impedance at high frequencies is caused by the ohmic resistance and corresponds to the model parameter $R_{\mathrm{s}}$.

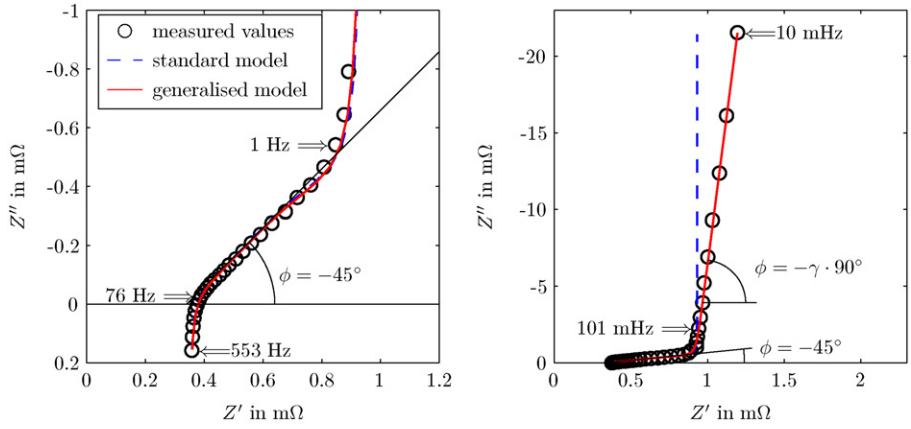


Fig. 2. Measured impedance spectrum (EPCOS 600 F, 25 °C, 2.7 $V_{\mathrm{dc}}$) and fitted spectra for the standard and generalised pore model, as described by Eqs. (4) and (7), respectively. The corresponding model parameters are given in Table 1. The aspect ratio of the right Nyquist plot has been changed to 1:10 in order to emphasise the deviation from true capacitive behaviour in the low frequency region.

### 2.2. Generalised pore impedance

However, a close observation of the low frequency branch of the impedance spectrum (Fig. 2, right part) reveals that the spectrum does not approach the behaviour of an ideal capacitor, as predicted by the standard pore model. Instead, a constant phase behaviour can be observed, however with an angle close to $-90\,^\circ$. This phenomenon was observed at EDLCs and other electrochemical systems and may arise from surface roughness [19], non-uniformity of the double layer thickness [20], a distribution in microscopic charge transfer rates or adsorption processes [3,21]. Pajkossy [22] and Kerner [23] have shown experimentally that even surface roughness on an atomic scale can produce such CPE behaviour. It is however not the scope of this paper to analyse these chemical processes in detail, but to develop mathematical models that describe the observed behaviour sufficiently.

Kötz et al. propose to replace the frequency-dependent terms ($j\omega$) in the expression for the pore impedance (Eq. (1)) by a constant phase term in the form $(j\omega)^\gamma$ with $0 < \gamma \leq 1$ [21]. The generalised expression for the pore impedance is

$$Z_{pg} = \sqrt{\frac{R_{el}}{(j\omega)^\gamma A_{dl}}}\ \coth\sqrt{(j\omega)^\gamma R_{el} A_{dl}}. \quad (5)$$

$C_{dl}$ in Eq. (1) was replaced by the term $A_{dl}$, the magnitude of the constant phase element (CPE).[1] Purely capacitive behaviour as in the standard pore model corresponds to $\gamma = 1$, $\gamma = 0.5$ would result in a $-45\,^\circ$ branch and $\gamma = 0$ describes purely resistive behaviour. The term $(j\omega)^\gamma A_{dl}$ is composed of a real part $\cos(\gamma\pi/2)\omega^\gamma A_{dl}$ and an imaginary part $\sin(\gamma\pi/2)\omega^\gamma A_{dl}$. In order to retrieve the true double layer capacitance, one can formally set $\omega C_{dl} = \sin(\gamma\pi/2)\omega^\gamma A_{dl}$. Unfortunately, the result is a frequency-dependent term:

$$C_{dl} = A_{dl}\,\omega^{\gamma-1}\sin(\gamma\pi/2). \quad (6)$$

However, for an EDLC, $\gamma$ is very close to 1, and for the relevant frequency range[2] the term $\omega^{\gamma-1}\sin(\gamma\pi/2) \approx 1$, thus the numerical values of $C_{dl}$ and $A_{dl}$ are nearly identical.

The complete impedance model for an EDLC including series resistance and inductance can be expressed in a closed expression:

$$Z_{EDLC} = R_s + j\omega L_s + \sqrt{\frac{R_{el}}{(j\omega)^\gamma A_{dl}}}\ \coth\sqrt{(j\omega)^\gamma R_{el} A_{dl}}. \quad (7)$$

This generalised model can be fitted very well to the measured spectrum of a real EDLC over the complete measured frequency range, as can be seen in Fig. 2. The model parameters for this example are given in Table 1.

Table 1
Example parameters of the impedance model (Eqs. (4) and (7)) for a commercial EDLC (cf. Fig. 2)

| Model | $R_s$ (mΩ) | $R_{el}$ (mΩ) | $L_s$ (nH) | $(F\,s^{(\gamma-1)})$ | $\gamma$ |
|---|---|---|---|---|---|
| Generalised | 0.34 | 1.77 | 51 | 729 | 0.992 |
| Standard[a] | 0.34 | 1.74 | 50 | 709 | 1.000 |

[a] For the determination of $R_s$, $R_{el}$ and $L_s$ the frequency range has been restricted to <100 mHz.

Table 2
Supercaps used in the accelerated ageing tests (all devices purchased in July and August 2004)

| Type | Manufacturer | Capacity (F) | Rated voltage (V) | Geometry | Datasheet |
|---|---|---|---|---|---|
| A | Epcos | 600 | 2.5 | Cylindrical | [26] |
| B | Nesscap | 600 | 2.7 | Prismatic | [27] |
| C | Maxwell | 350 | 2.5 | Cylindrical | [28] |

## 3. Experimental study of EDLC ageing

Even though energy storage in EDLCs is predominantly electrostatic,[3] parasitic electrochemical reactions limit the life expectancy of these devices. Decomposition of the electrolyte is one predominant factor; the composition of the electrode material has a strong impact on deterioration processes, Taberna et al. state that functional groups at the surface of the carbon electrode cause instability during ageing under floating at high potentials [24].

The two predominant factors that influence ageing in EDLCs are temperature and voltage. Both, increased voltage and temperature exponentially accelerate electrochemical reactions. The effect of this degradation is generally described as an increase of the internal resistance and a decrease of the capacitance of the devices [4,16,25].

### 3.1. Experimental setup

In order to quantify these effects and to analyse the effect of ageing on the parameters of the impedance model introduced in Section 2, three types of commercially available EDLCs from different manufacturers were analysed with respect to their ageing behaviour. Table 2 gives an overview of the devices under test.

Since the life expectancy of EDLCs under normal conditions, i.e. at voltages below the rated maximum voltage and at room temperature, is in the order of 10–20 years, ageing was accelerated by increasing voltage and temperature during the tests. According to a rule of thumb, the ageing rate doubles if either the cell voltage is increased by 100 mV or the temperature is

[1] The unit of $A_{dl}$ formally is $[A_{dl}] = s^\gamma\,\Omega^{-1} = F\,(s^{(1-\gamma)})^{-1}$. A physical meaning can yet only be assigned to the product $[\omega^\gamma A_{dl}] = \Omega^{-1}$.

[2] For frequencies above 10 Hz the contribution of the pore impedance to the total impedance is small. Frequencies below 10 mHz are of minor interest for the dynamic modelling of EDLCs. For significantly lower frequencies additional effects such as self-discharge have to be taken into account, which are not covered by the proposed model.

[3] Surface functional groups which are in general present on activated carbons account for a certain non-linear pseudocapacitance. The contribution in organic electrolytes, as for the devices tested in this study, is however small [21]. Pseudocapacitance is not incorporated explicitly in the models presented here, yet the impedance model allows a voltage-dependent parameterisation of the capacitance, which can be interpreted as the macroscopic effect of pseudocapacitance.

Table 3
Configuration for the ageing tests, voltages and temperatures with respect to rated voltage $V_r$ (cf. Table 2) and rated temperature $T_r = 25\,^{\circ}\mathrm{C}$ (≈298 K), respectively

| | $V_r + 200\,\mathrm{mV}$ | $V_r + 400\,\mathrm{mV}$ |
|---|---|---|
| $T_r + 20\,\mathrm{K}$ | B | A, B, C |
| $T_r + 40\,\mathrm{K}$ | A, B, C | A |

increased by 10 K. This was taken into account for the design of the tests.[4]

For each of the capacitor types two test conditions were chosen that should increase the ageing rate by a factor of approximately 64 by either increasing the temperature by 40 K above the nominal temperature of 25 °C (≈ 298 K) and the voltage by 200 mV above the rated voltage, or by an increase of 20 K and 400 mV, respectively. Thus, devices with a life expectancy of 15 years should reach their end of life within 3 months of test duration. Two additional tests were defined for types A ($V_r + 400\,\mathrm{mV}$, $T_r + 40\,\mathrm{K}$) and B ($V_r + 200\,\mathrm{mV}$, $T_r + 20\,\mathrm{K}$) in order to compare these devices at the same conditions, irrespective of their different voltage ratings (cf. Table 2). Table 3 summarises the test conditions for the three types of EDLCs.

The choice of voltage and temperature levels is crucial because values that differ too much from typical operating conditions could activate new electrochemical processes and cause atypical ageing behaviour. The temperature and voltage levels chosen for the tests are a compromise between this requirement and adequate test durations.

Two devices at a time were tested at the same conditions in order to avoid misinterpretation due to outliers. The devices were connected to a power supply in fully charged state at different test voltages and were held at constant ambient temperature in temperature chambers. The devices were only disconnected from the power supplies for regular impedance measurements and capacity tests and were directly recharged and reconnected afterwards. These performance tests were done in order to track the gradual change of the electrical behaviour during the ageing process. The impedance measurements were performed with the EISmeter, a multi-channel galvanostatic impedance spectrometer [29]. The measurements were conducted at the test voltages and test temperatures (cf. Table 3) in open circuit mode, i.e. without bias current, and in a frequency range from 5.25 kHz to 5.67 mHz.

Fig. 4 shows the development of the impedance spectra measured on a device of type A at 40 K above rated temperature and 200 mV above rated voltage with proceeding test duration. Some typical effects of the ageing process can be deduced directly from the spectra. The most prominent effect is a shift of the spectra along the real axis, corresponding to an increase of the internal resistance. It can also be seen that this process is fairly continuous during most of the test duration, but accelerates towards the end of the test. The last spectrum of the test is not shown in Fig. 4, its real part of the impedance is above 15 mΩ, indicating that the device is already severely damaged. All devices that reached this state during the tests showed such an acceleration of ageing after a certain level of degradation had been exceeded. However, the formal end of life, defined by an increase of the equivalent series resistance by a factor of 2, was always reached during the continuous ageing period.

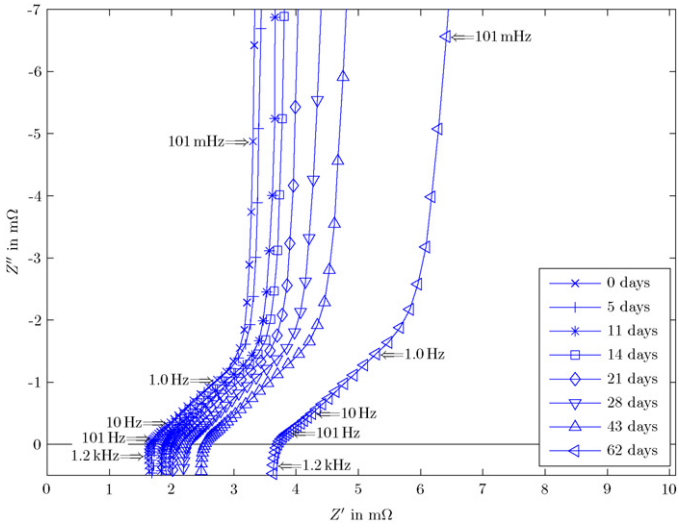


Fig. 4. Impedance spectra during progress of ageing for EDLC type A, test conditions: 65 °C, 2.7 V ($V_r + 200\,\mathrm{mV}$, $T_r + 40\,\mathrm{K}$).

Comparing measurement points at the same frequency in the capacitive branch in Fig. 4 shows that the imaginary part of the impedance at low frequencies also increases. Thus, the effective capacitance of the device decreases due to the ageing process. Both, the increase of the resistance and the decrease of the capacitance are in accordance with results from independent experimental analysis [4,25].

For a more detailed analysis of the ageing behaviour, the impedance model introduced in Section 2 was fitted to the measured impedance spectra.[5]

The model consists of a series resistance $R_s$, a stray inductance $L$ and a generalised pore impedance $Z_{pg}$. The generalised pore impedance is given in Eq. (5) and defined by three parameters, the pore electrolyte resistance $R_{el}$, the magnitude $A_{dl}$ of the constant phase element (CPE) and the CPE exponent $\gamma$. For an easier physical interpretation, the parameter $A_{dl}$ was equated with the double layer capacitance $C_{dl}$, as discussed in Section 2.

The result of the fitting procedure is a set of model parameters for each device and for each step of ageing. Spectra that showed extreme deterioration of the device ($R_s$ increased by more than a factor of 5) were excluded from analysis. Plotting the values along the test time axis allows analysing the effect of ageing on the model parameters. Fig. 5 shows the development of the model parameters with the progress of ageing for EDLCs of type A. The parameters prior to the ageing experiment (day 0) were determined at rated temperature $T_r$ and rated voltage $V_r$ for all

[4] Strictly exponential behaviour is always an approximation for a limited temperature and voltage range. In general, the activation energy itself is a function of temperature and especially high temperatures may introduce new chemical processes.

[5] The curve fitting was carried out with the mathematical software *Matlab*, using the function *easyfit* that is based on the Nelder–Mead simplex algorithm [30,31].

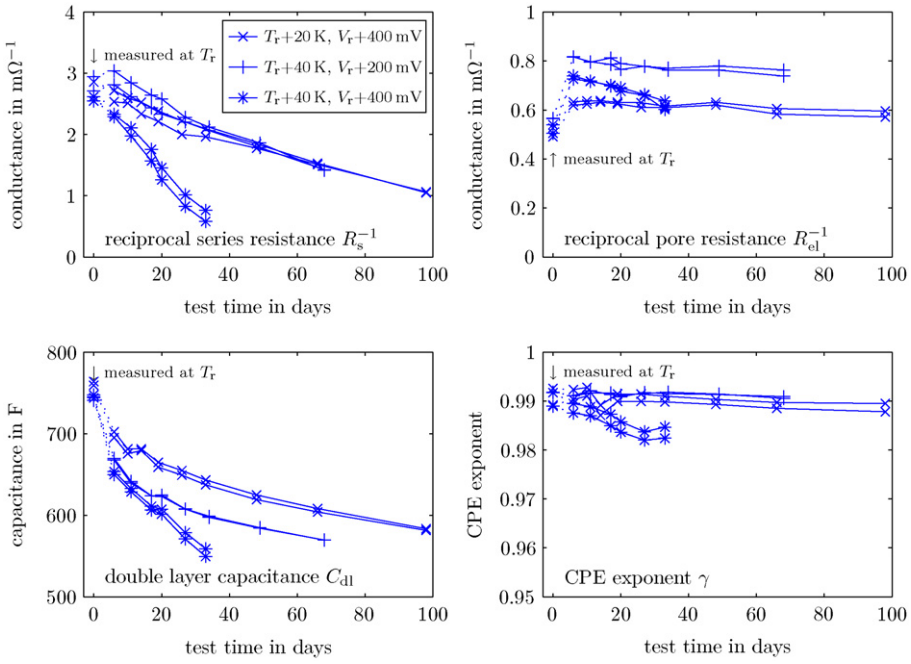


Fig. 5. Model parameters during accelerated ageing test for ageing, EDLC type A. $C_{dl}$ has been calculated according to Eq. (6) for $f$ =10 mHz. Note that the first measurement (before ageing) was conducted at rated temperature $T_r$ and rated voltage $V_r$ for comparison reasons.

devices, all other impedance measurements were carried out at the respective test temperature and voltage.

The two top figures show the reciprocal values of the series and pore electrolyte resistance. It was found that the conductances decrease nearly linearly with ageing time. The series conductance $R_s^{-1}$ shows a pronounced trend while the pore electrolyte conductance $R_{el}^{-1}$ is less sensitive to ageing. The double layer capacitance $C_{dl}$ also shows a noticeable decline of up to 20%. The CPE exponent that is correlated to the slope of the low frequency impedance branch, changes only little due to ageing. The series inductance showed relatively strong scattering but no clear trend. The inductance is mainly determined by the geometric design of the device, thus no ageing effect on $L_s$ is expected. Since the geometric inductance of EDLCs is very low (cf. Table 1), the stray inductance of the measurement cables contribute significantly to the measurement result and vary from test to test, but are not sensitive to ageing.

The parallel development of the model parameters obtained at $T_r + 20\,°C/V_r + 400\,mV$ and at $T_r + 40\,°C/V_r + 200\,mV$ corroborates the assumption that 10 K temperature rise and a voltage increase of 100 mV have virtually the same effect on the ageing behaviour of an EDLC.

A validated explanation of the ageing effects would require detailed electrochemical analysis that is beyond the scope of this work. A possible explanation for the fade of the double layer capacitance is a decrease of the active surface. Qualitatively the linear decrease of the conductance could also be assigned to a reduced cross-section surface, though the different slopes of $R_s$ and $C_{dl}$ prove that other effects contribute to the degradation. Weighing of the devices at the start and the end of the ageing test revealed that electrolyte was lost through the safety vents, which might have additional effects besides decomposition of the electrolyte.

### 3.2. Heuristic ageing model

As a working hypothesis for a heuristic ageing model, the following assumptions were made:

- At constant voltage and temperature, the capacitance and the conductance parameters decrease linearly with time.[6]
- The rate of degradation accelerates exponentially with temperature and voltage.[7]

The change of a model parameter $a$ compared to its initial value can thus be described by

$$a(t, T, V) = a_{init}(1 + c_a\, t_{eq}), \tag{8}$$

where $t_{eq}$ is the equivalent ageing time defined by

$$t_{eq} = t \cdot c_T^{(T-T_0)/\Delta T} \cdot c_V^{(V-V_0)/\Delta V}. \tag{9}$$

The constants $T_0$, $V_0$, $\Delta T$ and $\Delta V$ can be chosen arbitrarily. If $T_0$ and $V_0$ are set to rated temperature and voltage of the device, respectively, $t_{eq}$ equals the real time at nominal conditions and $c_a$ is the relative ageing rate at nominal conditions. For the results presented in the following, $T_0$ and $V_0$ were set to the rated values according to Table 2, $\Delta T$ to 10 °C and $\Delta V$ to 100 mV.

In order to determine the ageing model parameters $c_a$, $c_T$ and $c_V$ the model parameters that were obtained from the impedance

[6] A linear change was also assumed for the CPE exponent and the inductance in order to test for a correlation with ageing.

[7] The exponential dependency on the voltage is in good accordance with the Butler–Volmer equation. The reaction rate as it is described by Butler–Volmer or the basic Arrhenius equation increases exponentially with the negative inverse of the absolute temperature ($k \propto e^{-1/T}$). However, for a limited temperature range this can be approximated by an expression increasing directly exponentially with temperature.

Table 4
Parameters of the ageing model for an EDLC

| Type | Parameter | $c_a$ (in % year$^{-1}$) | $c_T$ | $c_V$ | $R^2$ | $\sigma_{err}$ |
|---|---|---|---|---|---|---|
| A | $R_s^{-1}$ | −6.94 | 1.98 | 1.75 | 0.98 | 0.033 |
| | $R_{el}^{-1}$ | −0.26 | 2.84 | 1.83 | 0.85 | 0.016 |
| | $A_{dl}$ | −6.81 | 1.66 | 1.44 | 0.93 | 0.018 |
| | $\gamma$ | −0.02 | 2.0[a] | 2.0[a] | 0.56 | 0.001 |
| B | $R_s^{-1}$ | −8.79 | 2.22 | 2.06 | 0.90 | 0.072 |
| | $R_{el}^{-1}$ | −4.60 | 2.0[a] | 2.0[a] | 0.51 | 0.145 |
| | $A_{dl}$ | −5.57 | 1.88 | 1.98 | 0.96 | 0.017 |
| | $\gamma$ | −0.42 | 2.0[a] | 2.0[a] | 0.42 | 0.012 |
| C | $R_s^{-1}$ | −5.20 | 2.0[a] | 1.92 | 0.99 | 0.022 |
| | $R_{el}^{-1}$ | −3.83 | 2.0[a] | 1.89 | 0.96 | 0.027 |
| | $A_{dl}$ | −2.03 | 2.0[a] | 1.94 | 0.98 | 0.015 |
| | $\gamma$ | −0.19 | 2.0[a] | 2.05 | 0.83 | 0.005 |

[a] Coefficient fixed during regression.

Table 5
Parameters of the simplified ageing model for an EDLC

| Type | Parameter | $c_a$ (in % year$^{-1}$) | $R^2$ | $\sigma_{err}$ |
|---|---|---|---|---|
| A | $R_s^{-1}$ | −4.11 | 0.96 | 0.089 |
| | $R_{el}^{-1}$ | −0.63 | 0.71 | 0.023 |
| | $A_{dl}$ | −1.12 | 0.80 | 0.031 |
| B | $R_s^{-1}$ | −12.07 | 0.90 | 0.151 |
| | $R_{el}^{-1}$ | −4.61 | 0.51 | 0.379 |
| | $A_{dl}$ | −4.69 | 0.96 | 0.023 |
| C | $R_s^{-1}$ | −4.54 | 0.99 | 0.052 |
| | $R_{el}^{-1}$ | −3.15 | 0.96 | 0.043 |
| | $A_{dl}$ | −1.83 | 0.98 | 0.017 |

spectra were fitted to the formula given in Eq. (8). Wherever possible, all parameters were left free for the regression analysis. Since the devices of type C were only tested at two operating points, $c_T$ and $c_V$ cannot be determined independently, $c_T$ was therefore fixed to a value of 2. Moreover, both $c_T$ and $c_V$ were set to a value of 2, where the regression did not converge or the correlation was too weak to produce reliable results for these parameters.

The results of the regression for all EDLCs in the ageing test are summarised in Table 4. As a measure for the quality of fitting, the coefficient of correlation $R^2$ and the standard deviation of the errors $\sigma_{err}$ are included. The results for the inductance were omitted due to the high scattering of the data and the very low correlation ($R^2 \ll 1$). The correlation for $\gamma$ is low for types A and B, the sensitivity to ageing is however very small, as can be seen from the values of $c_a$. The correlation for the inverse of the series resistance (which is the parameter that influences the dynamic performance of an EDLC most) is good, similarly the correlation for the linear decrease of the capacitance, expressed by the model parameter $A_{dl}$.

The fact that the influence of voltage and temperature on the deterioration rate can be described well by the exponential ageing model can also be interpreted as an indication that no new electrochemical processes have been activated.

The coefficients $c_T$ and $c_V$ are mostly close to a value of 2, as expected from the rule of thumb mentioned above. However, they vary not only from one EDLC type to another, but also for the different model parameters. In order to achieve a more simplified but also more consistent ageing model, all coefficients $c_T$ and $c_V$ were set equal to 2, which is close to the average of the regression results. Results of a regression with only $c_a$ as a free parameter are presented in Table 5. Except for type A the correlation coefficients are very close to those in Table 4. However, even for type A the simplified model describes the impact of ageing on the impedance parameters adequately, as can be seen in Fig. 6. The measurement points are the same as in Fig. 5 but normalized to the initial values of

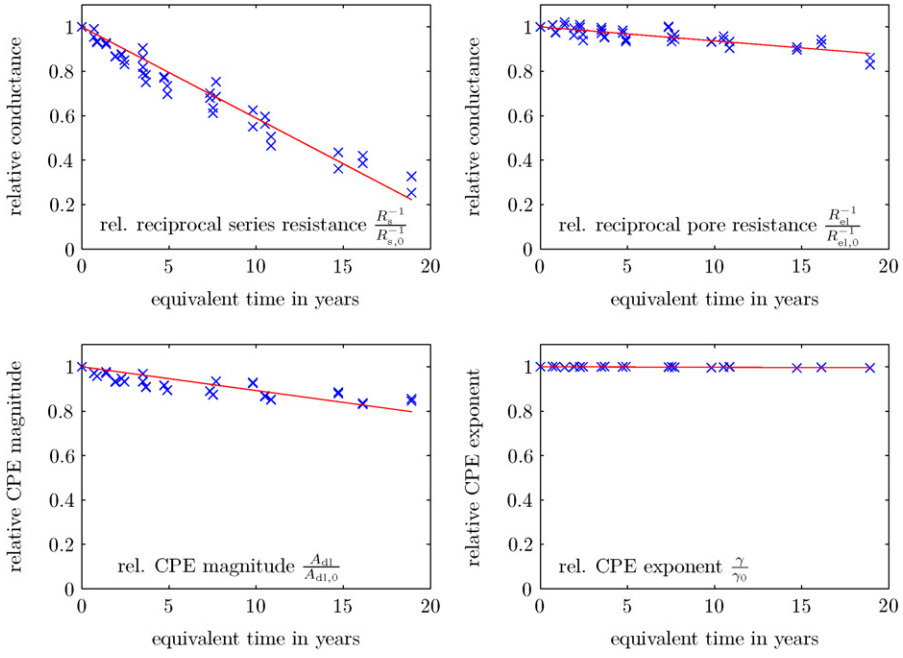


Fig. 6. Relative parameters for ageing, EDLC type A.

the new devices and plotted against the equivalent time $t_{eq}$. The lines mark the development described by the simplified ageing model with the parameters shown in Table 5.

For the interpretation of Tables 4 and 5, it should be kept in mind that type B has a rated voltage of 2.7 V, while that of the other two devices is only 2.5 V. This leads to ageing rates that seem significantly higher than the others. However, if $V_0$ for type B was set to 2.5 V, $c_a$ would be approximately one fourth of the value presented here. Thus, type B would age slightly slower if operated at the same conditions as types A and C, but its voltage was rated too high.

The development of commercial EDLCs is still a dynamic process, it is very likely that products available today show ageing rates different from the devices used in the tests, yet the dependency on temperature and voltage will be close to those presented here.

## 4. Conclusion

The electric behaviour of an EDLC can be described accurately with an impedance model composed of a series inductance, a resistance and a pore impedance. The generalised pore model that includes a variable constant phase component shows much better consistence with measurement data at frequencies significantly lower than 1 Hz than the standard pore model.

The change of the impedance parameters in the process of ageing can be described as a good first approximation by a linear decrease of conductances and capacitances. The change of the low-frequency CPE behaviour defined by $\gamma$ is less pronounced and shows a poorer correlation, the series inductance can be assumed to be constant.

An equivalent ageing time that depends exponentially on temperature and voltage has been introduced to model the ageing rate accordingly. This model allows an extrapolation of the results of the accelerated ageing tests towards lower voltage and temperature levels at normal operating conditions. The extrapolation towards potentials and temperatures far from the experimental conditions should however be made with great cautiousness, since different electrochemical reactions may dominate the deterioration process at low and high potentials and temperatures, respectively.

Ageing experiments were carried out at constant voltage and constant temperature conditions, the results can be generalised to dynamic operation under the assumption that these are the only relevant impact parameters. Possible impact of e.g. mechanical stress on the electrodes imposed by thermal cycles is not covered by this approach.

The changing electric behaviour of an EDLC due to ageing affects the internal heat generation and the voltage level during operation. These effects in turn influence the ageing itself, which can lead to self-accelerating processes. In Part II [32] a holistic simulation model is presented that combines the ageing model with an electrical and thermal model and allows the analysis of these feedback cycles as well as the influence of system design and operating conditions on the performance and ageing process of the devices.

## References

[1] C. Ashtiani, R. Wright, G. Hunt, J. Power Sources 154 (2) (2006) 561–566.
[2] A. Burke, M. Miller, Z. McCaffrey, Proceedings of the International Electric Vehicle Symposium (EVS), vol. 22, Yokohama, Japan, 2006, pp. 1385–1400.
[3] B.E. Conway, Electrochemical Supercapacitors: Scientific Fundamentals and Technological Applications, Kluwer Academic/Plenum Publishers, New York, 1999 (ISBN: 0-306-45736-9).
[4] R. Kötz, M. Hahn, R. Gallay, J. Power Sources 154 (2) (2006) 550–555.
[5] D. Linzen, S. Buller, E. Karden, R.W. De Doncker, Proceedings of the Industry Applications Conference, 2003, Conference Record of the 38th IAS Annual Meeting, vol. 3, 2003, pp. 1589–1595.
[6] EPCOS AG, UltraCap Technology, EPCOS AG, 2006.
[7] J.-N. Marie-Francoise, H. Gualous, A. Berthon, IEEE Proc. Electr. Power Applic. 153 (2) (2006) 255–262.
[8] H. Douglas, P. Pillay, Proceedings of the 32nd Annual Conference of IEEE Industrial Electronics Society, 2005 (IECON 2005), 2005.
[9] E. Karden, S. Buller, R.W. De Doncker, Electrochim. Acta 47 (13/14) (2002) 2347–2356.
[10] R. de Levie, Electrochim. Acta 9 (9) (1964) 1231–1245.
[11] E. Karden, Using low-frequency impedance spectroscopy for characterization, monitoring, and modeling of industrial batteries, Ph.D. Thesis, RWTH Aachen University, 2001.
[12] S. Buller, E. Karden, D. Kok, R.W. De Doncker, IEEE Trans. Ind. Applic. 38 (6) (2002) 1622–1626.
[13] S. Buller, M. Thele, R.W.A.A. De Doncker, E. Karden, IEEE Trans. Ind. Applic. 41 (3) (2005) 742–747.
[14] W. Lajnef, J.-M. Vinassa, O. Briat, S. Azzopardi, C. Zardini, Proceedings of the IEEE International Symposium on Industrial Electronics 2004, vol. 2, 2004, pp. 839–844.
[15] R.M. Nelms, D.R. Cahela, B.J. Tatarchuk, IEEE Trans. Aerospace Electr. Syst. 39 (2) (2003) 430–438.
[16] D. Linzen, Impedance-based loss calculation and thermal modeling of electrochemical energy storage devices for design considerations of automotive power systems, Ph.D. Thesis, RWTH Aachen University, Institute for Power Electronics and Electrical Drives ISEA,break 2006.
[17] D. Riu, N. Retiere, D. Linzen, Proceedings of the 39th IAS Annual Meeting on Industry Applications Conference, Conference Record of the 2004 IEEE, vol. 4, 2004, pp. 2550–2554.
[18] S. Buller. Impedance-based simulation models for energy storage devices in advanced automotive power systems, Ph.D. Thesis, RWTH Aachen University, Institute for Power Electronics and Electrical Drives ISEA, 2002.
[19] R. de Levie, Electrochim. Acta 10 (2) (1965) 113–130.
[20] M.F. Mathias, O. Haas, J. Phys. Chem. 97 (36) (1993) 9217–9225.
[21] R. Kötz, M. Carlen, Electrochim. Acta 45 (15/16) (2000) 2483–2498.
[22] T. Pajkossy, Solid State Ionics 176 (25–28) (2005) 1997–2003.
[23] Z. Kerner, T. Pajkossy, Electrochim. Acta 46 (2/3) (2000) 207–211.
[24] P.-L. Taberna, G. Chevallier, P. Simon, D. Plee, T. Aubert, Mater. Res. Bull. 41 (3) (2006) 478–484.
[25] A. Schneuwly, M. Bärtschi, V. Hermann, G. Sartorelli, R. Gallay, R.Kötz, Proceedings of the Advanced Automotive Battery Conference (AABC), 2002, pp. 1/15–15/15.
[26] EPCOS AG, UltraCap 600 F/2.5 V (B49410-A2605-Q000) datasheet, EPCOS AG, 2004.
[27] Nesscap, Ltd., NESSCAP 600 F/2.7 V (ESHSP-0600C0-002R7) datasheet, Nesscap, Ltd., 2004.
[28] Maxwell Technologies SA, BOOSTCAP 350 F/2.5 V (BCAP0350-A01) datasheet, Maxwell Technologies SA, 2004.

[29] H. Blanke, O. Bohlen, S. Buller, R.W. De Doncker, B. Fricke, A. Hammouche, D. Linzen, M. Thele, D.U. Sauer, J. Power Sources 144 (2) (2005) 418–425.
[30] J.C. Lagarias, J.A. Reeds, M.H. Wright, P.E. Wright, SIAM J. Optim. 9 (1) (1998) 112–147.
[31] The Mathworks, Inc., Documentation for MathWorks Products, The Mathworks, Inc., http://www.mathworks.com, 2006 (accessed October 2006).
[32] O. Bohlen et al., J. Power Sources (2007) doi:10.1016/j.jpowsour.2007.07.059.